Progress In Electromagnetics Research M, Vol. 120, 135–144, 2023

Design and Optimization of 2D Photonic Crystal Based Compact All Optical T Splitter for Photonic Integrated Circuits

Poonam Jindal and Aarti Bansal*

Abstract—An all-optical compact polarization T splitter based on 2-dimensional photonic crystal with uniform structural and bandgap characteristics is proposed in this paper. A square lattice of silicon substrate with embedded air holes is used to create the proposed structure. Linear waveguides with 90° bends are created for light propagation by removing a number of holes to build the structure. Plane Wave Expansion (PWE) and Finite Difference Time Domain (FDTD) methods are employed for simulating the structure. The transmittance of transverse electric (TE) polarized mode at 1550 nm is 96%. The structural parameters, such as air hole radius and dielectric constant, are homogeneous throughout the structure, making production easier and reducing fabrication errors. The proposed polarization splitter has a simple design with small footprints and high Q factor to meet the demands of current optical integrated circuits.

1. INTRODUCTION

Photonic crystals (PCs) are tiny artificial structures in which alternate layers of dielectric constant regulate the flow of light. Photons (light particles) will convey and store data within these structures, just as electrons do on traditional semiconductor chips [1]. PCs according to researchers will infiltrate every aspect of electronics, from mobile phones to computers, making them compact, faster, and more efficient. PCs are a revolution in optical technology and will reduce the size of a wide range of optical devices by at least 1000 times [2]. PCs will begin enhancing and complementing electrical semiconductor technologies in less than a decade and may eventually replace them entirely [3]. Electrons are channeled through electronic gates or transistors when data is transferred on silicon chips. These charged particles interact with one another in close proximity, generating extreme heat and restricting their movement [4]. On the other hand, PCs, which employ uncharged photons to transmit data, have the potential to break this barrier. These are highly ordered microstructures like a checkerboard pattern made of semi-transparent materials like silicon or glass and might resemble a solid box stacked with hollow balls. Each ball is 1000 times smaller than the hair of a human, with a diameter that corresponds to the wavelength of light. Like becoming lost in a mirror maze, light shined into the crystal is imprisoned by its highly structured microstructure but with the insertion of defects, PCs truly sparkle [5]. Altering ball dimensions or the chemical microstructure of PC creates the defects. These defects operate as efficient light guides, guiding light along chosen directions. The directed light travels at a far faster rate than electrons in a semiconductor which results in sophisticated optical features such as light switches, filters, beam splitters, logic gates, and even mini-lasers [6, 7]. Although PCs are theoretically well understood, producing precisely consistent structures on such small dimensions remains a significant challenge. Maxwell's equations are considered for studying propagation of light in periodic structures

Received 8 August 2023, Accepted 20 October 2023, Scheduled 2 November 2023
* Corresponding author: Aarti Bansal (aarti.bansal@chitkara.edu.in).
The authors are with the Chitkara University Institute of Engineering and Technology, Chitkara University, Punjab 140 401, India.

as shown in Eq. (1) [8].

$$\nabla \cdot B = 0 \tag{1}$$

$$\nabla \cdot D = \rho \tag{2}$$

$$\nabla \times E = -\frac{\partial B}{\partial t} \tag{3}$$

$$\nabla \times H = J + \frac{\partial B}{\partial t} \tag{4}$$

where B is the flux density, J the displacement vector, ρ the free charge density, and J the conduction current. H and E signify the magnetic and electric field vectors, respectively. In various optical communication systems, adequate functionality and realization of PC based devices with decreased area and excellent power efficiency are required. Optical filters, multiplexers and demultiplexers, switches, couplers, power splitters, sensors, flip flops, and various types of logic gates are developed in recent years using two-dimensional PCs [9–13]. One of the most important optical devices for the development of photonic integrated chips is power splitter. It is an important component for bridging the gap between the various sections of an integrated optical device [14]. Many high-throughput power splitter designs have been presented in recent years [14–17]. Thus, the unique design properties of PC structure has a great influence on the functionality of power splitters that depend upon lattice parameters and covers wavelength specific bandgap and fabrication methods. However, the size of these structures for implementation in photonic integrated circuits is the key restriction, and their capacity to tune to a single wavelength is an issue. In [18] by Fan et al., TM polarized T waveguide branches in 2D PC of dielectric rods in air are discussed. A transmission efficiency of 44.4% is achieved by optimizing the cavity with point defect. In [19] by Gannat et al., Finite Difference Time Domain (FDTD) technique is employed to design different T splitter configurations. Use of reflectors along with the structure resulted in a noticeable enhancement in the functioning of the device. A multi-port splitter in the size range of 80–100 μm^2 is designed by Lerer et al. in [20]. T-type, Y-type, and line defect waveguide configurations integrated with multimode interference (MMI) are reported for telecommunication purpose with a transmission efficiency of 92.8% for T-type splitter. In [21] by Mohammadi and Mansouri-Birjandi, cavity resonators are designed among the five ports of a T-splitter to maintain an appropriate separation between the ports to minimize direct coupling. MMI effect is introduced, and refractive coefficient and radius of rods in the cavity are varied to obtain high output efficiency. Despite having good transmission efficiency, the power splitters suggested in the cited publications have certain manufacturing challenges because of their design complexity [22]. Further, it is observed that the PC splitters devised recently suffer from large device size, low transmission efficiency, and exhibit operational wavelength in higher attenuation window [23–26]. In addition, it is seen that some of the designed structures are based on elliptical air holes that leads to fabrication complexity.

The major contributions of this article are given as follows-

1. A 1×2 T splitter is proposed with line defects on a PC based 2D square lattice.
2. The proposed device has ultra-compact dimensions suitable for photonic integrated circuits (PICs).
3. Moreover, the simple and symmetrical design of the proposed splitter results in uniform distribution of power and leads to low fabrication complexity.
4. The complete methodology adopted to design the optical power splitter is well illustrated in Figure 1.
5. The designed splitter is highly suitable for implementation in all optical processors and photonic integrated circuits for uniform distribution of power.

The manuscript is structured as follows. In Section 2, the band diagram and calculation of bandgap are given. The design of the proposed T splitter is presented in Section 3. Section 4 discusses the results. Finally, the potential of power splitter in photonic integrated circuit applications is summarized in Section 5.

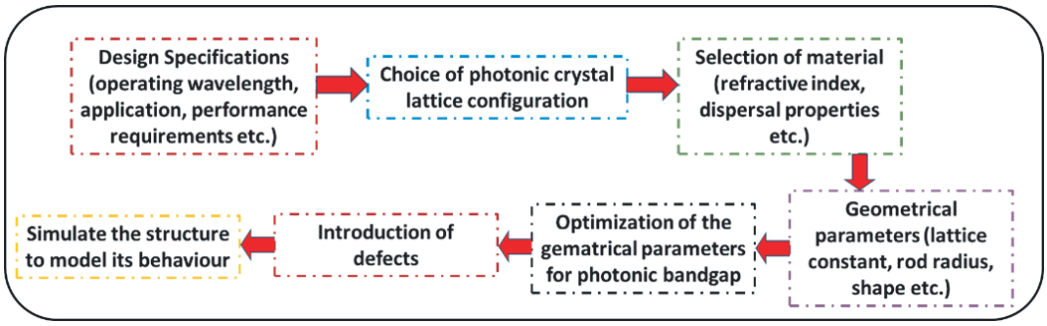

Figure 1. Methodology to design a photonic crystal-based power splitter design.

2. CALCULATION OF BANDGAP

The proposed T splitter is designed using dielectric rods placed in the X-Z direction. It consists of a silicon (Si) substrate with a refractive index (RI) of 3.1, and air holes are embedded in it with an RI of 1. The propagation of electromagnetic (EM) modes in the absence of defects for TE polarization is shown in the band diagram of Figure 2. The dimensional parameters that are considered are the radius of rods (r), lattice constant of air holes (a) (the distance between the center of two air holes), and filling factor (r/a). Therefore, the parameter values are 0.2 µm, 1 µm, and 0.2, respectively. The investigation of the photonic bandgap (PBG) is done with the plane wave expansion (PWE) method. The air hole periodic structure is expanded in the Fourier series, and the calculated band gap lies in the first Brillouin Zone (BZ). In k space Γ- and M-K points are used to obtain the values of x-axis, and normalized frequency ($\omega a/2\pi c = a/\lambda$) is plotted along z axis. From the combination of Eqs. (2) and (4) wave equation is completely written in $H(r)$ as shown in Eq. (5) [27]:

$$\nabla \times \frac{1}{\varepsilon(r)} \nabla \times H(r) = \left(\frac{\omega}{c}\right)^2 H(r) \tag{5}$$

where $c = 1/\sqrt{\varepsilon_0 \mu_0}$ and is the velocity of light in free space; $\varepsilon(r)$ is the permittivity of the material; and ω is the angular frequency. All the properties of $H(r)$ are defined by the master equation (Eq. (5)) along with transversality, and the obtained band diagram is actually its solution. The equation explains the propagation of light inside the periodic structure without significant scattering and results from Bloch-Floquet theorem [28]. The central wavelength (λ_c) of the band-gap is expressed in Eq. (6) and is calculated based on the refractive index and dimensions of the structure. With n_1/n_2, a/b, and the lattice constant of PC, $l = a + b$, the central wavelength can be determined as follows:

$$\lambda_c = \frac{2(n_1 \times a + n_2 \times b)}{m} = 2n_2 \frac{l}{1 + \frac{a}{b}} \left(\frac{n_1}{n_2} \times \frac{a}{b} + 1\right) \frac{1}{m} \quad m = 1, 2, 3, \ldots \tag{6}$$

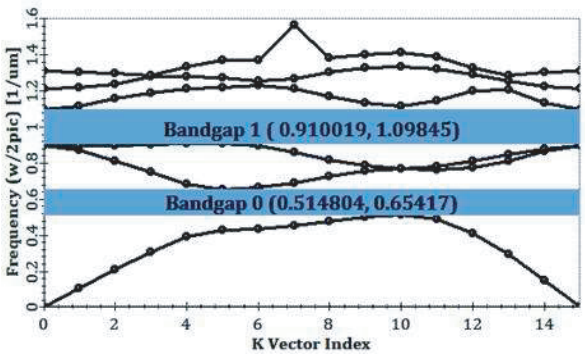

Figure 2. Photonic bandgap of the proposed 2D square lattice structure of T splitter.

where n_1 and n_2 are the refractive indices, and a and b are the thicknesses of the two dielectric materials used for designing the 2D crystal. For TE mode, the range of frequency lies between $0.514804 \leq a/\lambda \leq 0.65417$ equivalents to wavelength range of 1550 nm $\leq \lambda \leq$ 1940 nm that corresponds to optical communication low loss window. The results demonstrate that the T splitter is perfect for the third communication window ($\lambda = 1550$ nm) and is apt for photonic integrated circuits (PICs).

3. T-JUNCTION SPLITTER DESIGN

The PC structure with square lattice is composed of a Si substrate with a periodic array of circular air holes for designing the T splitter on OptiFDTD software. The number of holes in the 'X' and 'Z' directions are periodically arranged in a 10×10 square configuration array as shown in Figure 3(a).

2D PC lattice consists of a periodic arrangement of holes in 'X' and 'Z' directions whereas it is non-periodic in the 'Y' direction. The typical examples include: a periodic arrangement of dielectric rods in the air and air holes spaced in a dielectric block [29]. The performance of the splitter mainly depends on the geometry and location of the air holes inside the PBG structure. The incident light reaching the output ports is maximized by varying the radius and RI of the scattering holes. This structure consists of waveguides with 90° bend in a slab of size 10 µm × 10 µm as shown in Figure 3(b). At input port, x and y-oriented plane waves at 1.5 µm are coupled to the optimized geometry of the PC structure. A Gaussian signal given at the input port travels into the waveguide structure.

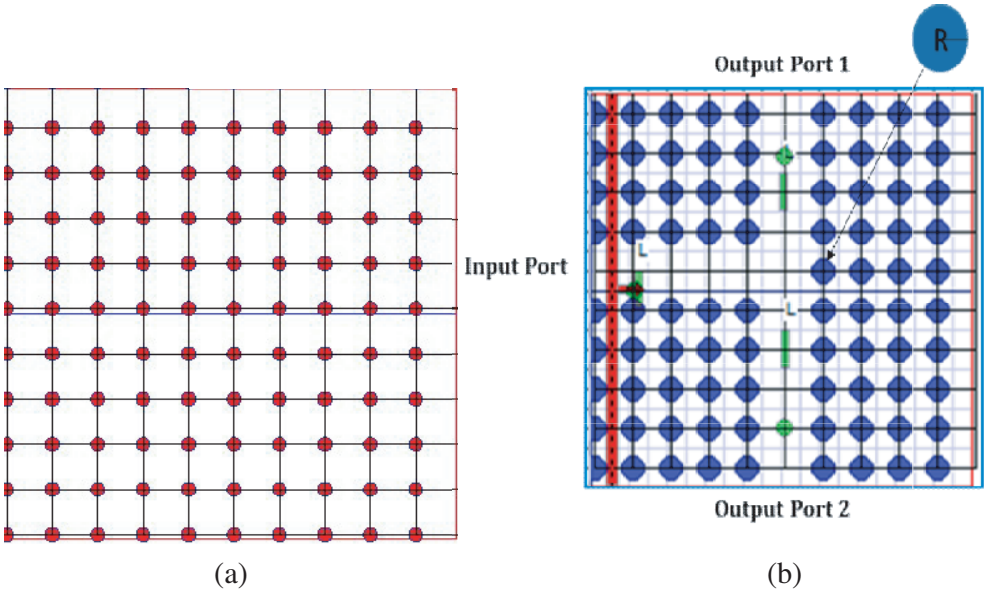

Figure 3. Schematic diagram, (a) 10×10 structure without defects, (b) T-junction splitter structure with input and output waveguide.

4. RESULTS AND DISCUSSION

The analysis and modelling of the designed splitter are carried out using the OptiFDTD tool. Plane wave expansion (PWE) method and Finite Difference Time Domain (FDTD) techniques are employed to obtain the photonicbandgap and powerspectrum analysis of the proposed splitter. The parameters considered for simulating the device are given in Table 1. The variation of the air hole radius from 0.5 to 3.2 µm results in changes in the wavelength from 1550 to 1940 nm. Thus, the wavelength of the T-junction moves towards third optical window by increasing the radius of air holes. Moreover, the symmetry of the structure is another significant parameter in the design of proposed splitter and results in the same amount of power distribution across output ports 1 and 2 as shown in the contour map of electric field distribution in Figure 4.

Table 1. Parameters for FDTD simulation.

Parameters	Value
Polarization	Transverse Electric (TE)
Operating Wavelength	1.55 µm
Mesh size in the X-axis	0.2 µm
Mesh size in the Y-axis	0.2 µm
Mesh cell count x	225
Mesh cell count z	225
Input Field	Gaussian
Boundary condition	Perfectly Matched Layers

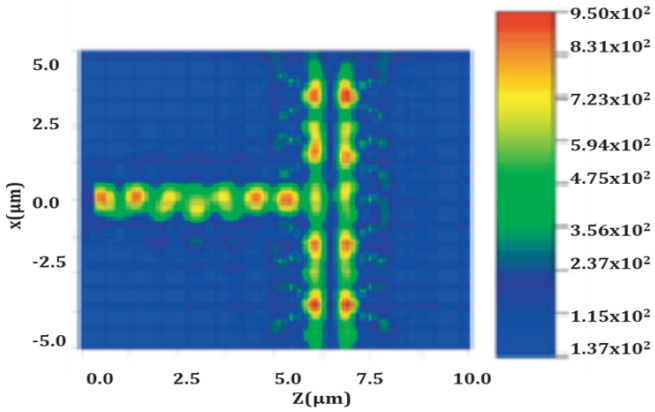

Figure 4. Distribution of Electric field (V/m) inside the waveguide structure at 1550 nm along z-direction.

The quality factor is defined as the ratio of centre wavelength (λ_c) to bandwidth ($\Delta\lambda$) and expressed by the Eq. (7) as follows:

$$Q = \frac{\lambda_c}{\Delta\lambda} \tag{7}$$

The quality factor and transmission efficiency based on the variations in the radius of holes are plotted in Figure 5. It is observed from the figure that the maximum value of quality factor and transmission efficiency are found to be 900 and 96% respectively at the optimum radius of 2 µm.

As the RI of the substrate material changes in the lattice structure from 2.6 to 3.2, the output wavelength varies from 1554 to 1556 nm and maximum power transmission achieved at 1550 nm for an RI of 3.1 as illustrated in Figure 6.

The input light is excited from the input port using the control parameters at a specific wavelength. The transmitted power is determined by integrating the Poynting vector over the output port cells using Eq. (8) [25].

$$P = \frac{1}{2}\mathrm{Re}\left[\int [E(t) \times H(t)] \cdot \overrightarrow{dA}\right] \tag{8}$$

The output sensitivity is determined by calculating the changes in the per channel wavelength based on the radius of inner holes using Eq. (9) and is represented in Figure 7.

$$S = \frac{\Delta\lambda}{\Delta r} \tag{9}$$

where $\Delta\lambda$ indicates the change in the resonant wavelength of the ports, and Δr is the variation air hole radius [30]. The optimum value of radius of air holes for the highest sensitivity is observed to be 2 µm.

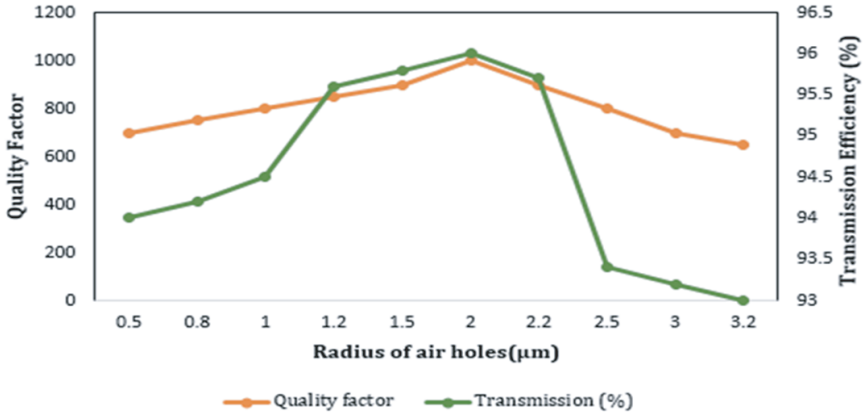

Figure 5. Quality factor and transmission efficiency for varying radius of the air holes.

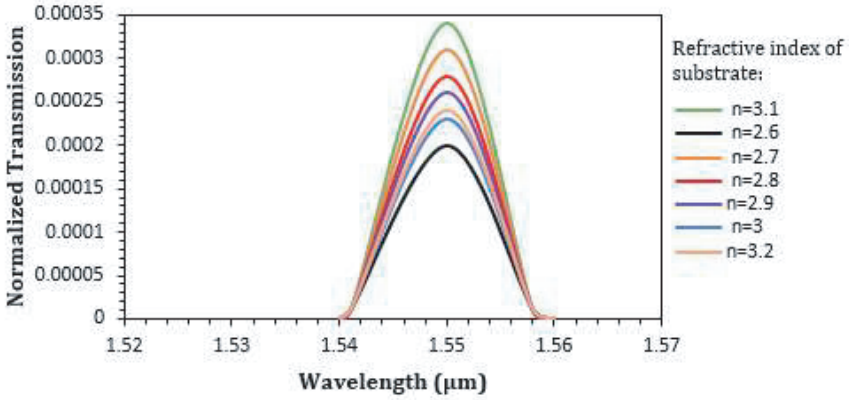

Figure 6. Normalized transmission for different RI of the substrate.

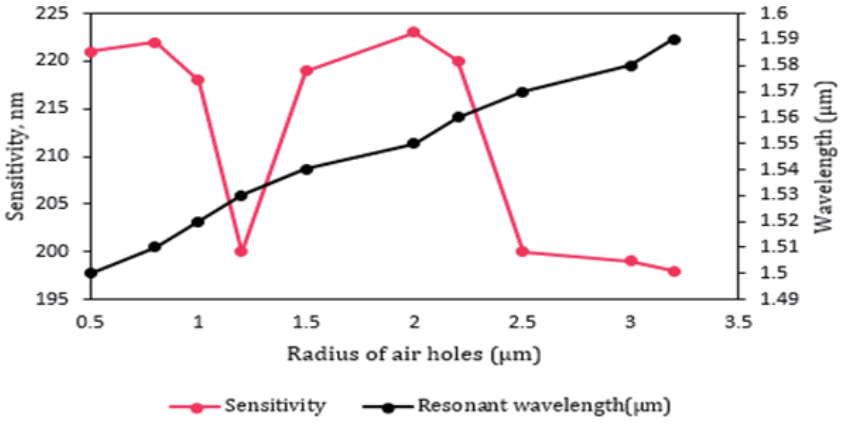

Figure 7. Sensitivity and resonant wavelength variations for different radius of holes.

Light signal of 1 μV is launched into the input port, and the corresponding output power at different wavelengths is shown in Figure 8.

It is evident that better optical power spitting is obtained at 1550 nm than other wavelengths. According to FDTD results, the highest transmission at 1550 nm for each port is 97% and 92%. To overcome the reflections at the boundary, the boundary condition of the perfectly matched layer (PML)

is employed [31]. All incident energy is absorbed by the PML without being reflected. This made it possible for field energy that strikes the barrier to escape the domain efficiently. In the simulation, the PML border condition has a width of 500 nm. The grid sizes (Δx, Δz) for FDTD calculations are equal to 0.02 µm. The stability criteria specified by the inequality must be satisfied by time step in order to produce precise and stable results [32]:

$$\Delta t \leq \frac{1}{c\sqrt{\frac{1}{\Delta x^2} + \frac{1}{\Delta z^2}}} \tag{10}$$

where c is the velocity of light in free space, and time step Δt is equal to 0.01 ns in Eq. (10).

Fundamentally, the constructive interference is the primary reason that the normalized optical power is greater than 1.0. It is created under resonance conditions inside the waveguide structure. Positive interference causes the input light signals (splitting at the junction) to be added in phase, creating waves with high power at the output ports. Table 2 presents the essential parameters like operating wavelength and output power of the proposed splitter.

Table 2. Optical transmission efficiency and quality factor of the proposed two port 2D PC T-splitter.

Output Port	Wavelength (µm)	Transmission Efficiency (%)
Port 1	1.55	97
Port 2	1.55	92

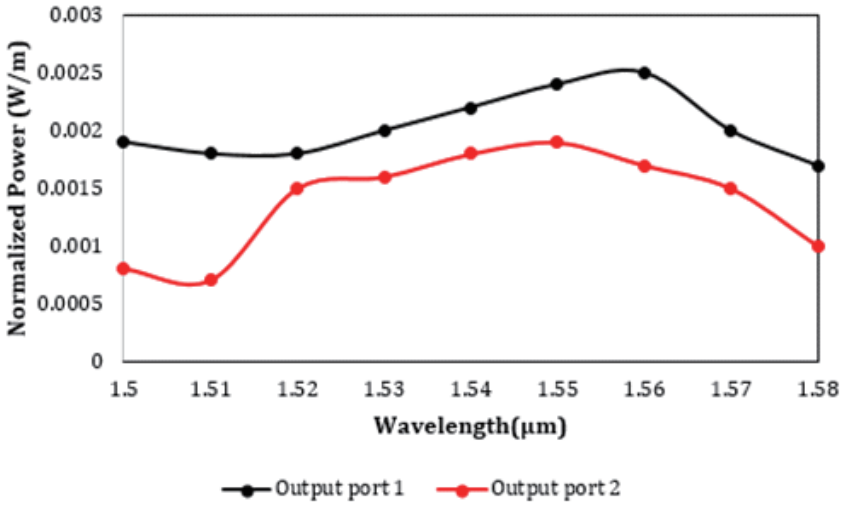

Figure 8. Normalized power transmission variations against wavelength inside the splitter.

As shown in Table 2, output observed at port 1 and port 2 exhibits transmission efficiency of 97% and 92%, respectively.

Table 3 compares the key parameters (device size, number of ports, wavelength and transmission efficiency, and type of dielectric) of the proposed structure to the recently presented all-optical splitters by various researchers.

The proposed splitter exhibits compact footprint as compared to devices presented [24, 26, 33, 34] and has a better transmission efficiency than devices in [23, 25, 26, 35]. Besides, the device designed in [23, 25] employed elliptical and square shaped rods that are difficult to design and fabricate. Hence, the designed all-optical compact two-port splitter has very desirable line width, spacing between the channels, transmission efficiency, and quality factor compared to the devices proposed in the literature

Table 3. Comparison of the proposed all-optical compact two-port T splitter with the reported ones.

References	Device size (μm^2)	Number of Ports	Wavelength (μm)	Transmission Efficiency (%)	Type of dielectric	Findings
Yong-Feng Gao et al. [23]	-	2	150.9–153.7	> 90	Elliptical rods	• Fabrication is more challenging and complex for elliptical rods • Increased design complexity • Limited wavelength range
S. Geerthana et al. [24]	315	2	1.99	-	Circular air holes	• Decreased Compactness • Added Fabrication Complexity • Enhanced Material Requirements
Dan Liu et al [25]	84.6	2	1.55	94.9	Circular and square air holes	• Unsymmetrical structure • Complication in design and simulation
T. Sridarshini et al. [26]	109.35	2	1.49	87.12	Circular dielectric rods	• Low transmission efficiency • Narrow operating wavelength range
R. Rajasekar et al. [33]	179	5	1518.4	0.841 mW	Circular dielectric rods	• Large device size • Non symmetrical structure
Purnamaningsih et al. [34]	100	8	0.45	-	-	• Complex design • Fabrication complexity
M. Boulesbaa et al. [35]	-	3	1.55	92	Circular air holes	• Anisotropic behaviour • Limited dispersion control
Proposed Structure	100	2	1.55	96	Circular air holes	• Symmetrical Structure • Ultra Compact Dimensions • Simple Design with low complexity • Structure with uniform air hole radius

[23–26, 33–35]. Thus, the designed device is well suited for photonic integrated circuit applications. Further, such devices based on photonic crystal technologies are targeted to make a huge impact on the chip fabrication industry by replacing traditional chips with ultra-compact photonic chips with fast processing capability. Some of the challenges to develop such devices are fabrication compatibility with standard CMOS processes, low insertion loss, scalability, and nano fabrication methods.

5. CONCLUSION

This paper presents the structural design for a 2D PC T-splitter. The layout of the proposed optical T-splitter consists of a square lattice with air holes etched on a silicon chip. Also, line defects are introduced by removing air holes in the input and output part. This is done in order to divide power into two output ports and reduce radiation losses. The bandgap and normalized power distribution are then calculated using the PWE and FDTD method. The simulation results depict that the proposed splitter has ultra-compact dimensions and high transmission efficiency of 96%. Thus, the simple and symmetrical structure of the splitter is highly suitable for optimal utilization in optical communication and photonics integrated circuits. Moreover, devices utilizing photonic crystal technologies have the potential to revolutionize the chip fabrication industry by replacing conventional chips with extremely compact photonic counterparts possessing fast processing capabilities. Additionally, these power splitters are critical components of photonic integrated circuits, which are used in wavelength-division multiplexing (WDM) systems, optical switches, and routers, among other applications for optical signal processing.

REFERENCES

1. Goyal, R., "Introduction to nanomaterials and nanotechnology," *Nanomaterials and Nanocomposites*, 2018, doi: 10.1201/9781315153285-1.
2. Yablonovitch, E., "Photonic crystals," *J. Mod. Opt.*, Vol. 41, No. 2, 173–194, 1994, doi: 10.1080/09500349414550261.
3. Joannopoulos, J. D., S. G. Johnson, J. N. Winn, and R. D. Meade, *Photonic Crystals: Molding the Flow of Light*, 2nd Edition, 2008.
4. Yablonovitch, E., "Photonic crystals: Semiconductors of light," *Scientific American*, 2001, doi: 10.1038/scientificamerican1201-46.
5. Seydou, F. and T. Seppänen, *Photonic Crystals: from Theory to Practice*, 2001.
6. Takahashi, H., "Planar lightwave circuit devices for optical communication: Present and future," *Act. Passiv. Opt. Components WDM Commun. III*, Vol. 5246, 520, 2003, doi: 10.1117/12.512904.
7. Kaur, H. J., "Comparison of light absorption through biological tissue implanted with gold and silver nano-particles," *J. Opt.*, Vol. 51, No. 3, 613–619, 2022, doi: 10.1007/s12596-022-00864-6.
8. Pain, H. J., "Electromagnetic waves," *The Physics of Vibrations and Waves*, 2005, doi: 10.1002/0470016957.ch8.
9. Jaskorzynska, B., Z. J. Zawistowski, M. Dainese, J. Cardin, and L. Thylen, "Widely tunable directional coupler filters with 1D photonic crystal," *Proceedings of 2005 7th International Conference Transparent Optical Networks, 2005*, 136–139, 2005.
10. Rao, D. G. S., S. Swarnakar, and S. Kumar, "Design of photonic crystal based compact all-optical 2×1 multiplexer for optical processing devices," *Microelectronics J.*, Vol. 112, 105046, 2021, doi: 10.1016/j.mejo.2021.105046.
11. Park, D. S., J. H. Kim, B. H. Oo, S. G. Park, E. H. Lee, and S. G. Lee, "Design of photonic crystal-based THz devices: Power splitter and demultiplexer," *Pacific Rim Conf. Lasers Electro-Optics, CLEO — Tech. Dig.*, Vol. 443, 0–1, 2007, doi: 10.1109/CLEOPR.2007.4391796.
12. Zhang, Y., Y. Zhang, and B. Li, "Optical switches and logic gates based on self-collimated beams in two-dimensional photonic crystals," *Opt. Express*, Vol. 15, No. 15, 9287, 2007, doi: 10.1364/oe.15.009287.
13. Veisi, E., M. Seifouri, and S. Olyaee, "Design and numerical analysis of multifunctional photonic crystal logic gates," *Opt. Laser Technol.*, Vol. 151, 108068, 2022, doi: 10.1016/j.optlastec.2022.108068.
14. Saral, T. B., S. Robinson, and R. Arunkumar, "Two-dimensional photonic crystal based compact power splitters," Vol. 2, 1–5, 2016.
15. Butt, M. A., S. N. Khonina, and N. L. Kazanskiy, "Recent advances in photonic crystal optical devices: A review," *Opt. Laser Technol.*, Vol. 142, 107265, 2021, doi: 10.1016/j.optlastec.2021.107265.
16. Arunkumar, R., J. K. Jayabarathan, and S. Robinson, "Design and analysis of optical Y-splitters based on two-dimensional photonic crystal ring resonator," *Journal of Optoelectronics and Advanced Materials*, Vol. 21, No. 7–8, 435–442, 2019.
17. Kaur, H. J. and Phalguni, "Design and analysis of single loop and double loop photonic crystal ring resonator based on hexagonal lattice structure," *Optik (Stuttg)*, Vol. 179, 165–172, 2019, doi: 10.1016/j.ijleo.2018.10.157.
18. Fan, S., S. G. Johnson, and J. D. Joannopoulos, "Waveguide branches in photonic crystals," *Journal of the Optical Society of America B*, Vol. 18, No. 2, 162–165, 2001.
19. Gannat, G. A., D. Pinto, and S. S. A. Obayya, "New configuration for optical waveguide power splitters," *IET Optoelectronics*, Vol. 3, No. 2, 105–111, April 2009, doi: 10.1049/iet-opt.2008.0020.
20. Lerer, A. M., I. V. Donets, and S. M. Tsvetkovskaya, "Study of wave propagation in two-dimensional photonic crystal," *Proceedings of International Seminar/Workshop on Direct and Inverse Problems of Electromagnetic and Acoustic Wave Theory, DIPED*, 63–65, 2016, doi: 10.1109/DIPED.2016.7772214.

21. Mohammadi, M. and M. Mansouri-Birjandi, "Five-port power splitter based on pillar photonic crystal," *Iran. J. Sci. Technol. Trans. Electr. Eng.*, Vol. 39, No. E1, 93–100, 2015, doi: 10.22099/ijste.2015.3063.
22. Cheng, C. C., "New fabrication techniques for high quality photonic crystals," *J. Vac. Sci. Technol. B Microelectron. Nanom. Struct.*, Vol. 15, No. 6, 2764, 1997, doi: 10.1116/1.589723.
23. Gao, Y. F., et al., "Manipulation of topological beam splitter based on honeycomb photonic crystals," *Opt. Commun.*, Vol. 483, 126646, 2021, doi: 10.1016/j.optcom.2020.126646.
24. Geerthana, S. and S. Syedakbar, "Design and optimization of Y-Junction and T-Junction splitters using photonic crystal," *Mater. Today Proc.*, Vol. 45, Part 2, 1722–1725, 2021, doi: 10.1016/j.matpr.2020.08.617.
25. Liu, D., D. S. Citrin, and S. Hu, "Compact high-performance polarization beam splitter based on a silicon photonic crystal heterojunction," *Opt. Mater. (Amst).*, Vol. 109, 110256, 2020, doi: 10.1016/j.optmat.2020.110256.
26. Sridarshini, T., I. G. S., and M. Rakshitha, "Design and analysis of 1xN symmetrical optical splitters for photonic integrated circuits," *Optik (Stuttg)*, Vol. 169, 321–331, 2018, doi: 10.1016/j.ijleo.2018.05.053.
27. Yee, K. S., "Numerical solution of initial boundary value problems involving Maxwell's equations in isotropic media," *IEEE Transactions on Antennas and Propagation*, Vol. 14, No. 3, 302–307, 1966, doi: 10.1109/TAP.1966.1138693.
28. Johnson, S. G. and J. D. Joannopoulos, "Introduction to photonic crystals: Bloch's Theorem, Band Diagrams, and Gaps (But No Defects) Maxwell's Equations in periodic media," *Physics*, 1–16, February 2003.
29. Reynolds, A. L., U. Peschel, F. Lederer, P. J. Roberts, T. F. Krauss, and P. J. I. De Maagt, "Coupled defects in photonic crystals," *IEEE Trans. Microw. Theory Tech.*, Vol. 49, No. 10, 1860–1867, 2001, doi: 10.1109/22.954799.
30. Hou, J., M. Li, and Y. Song, "Recent advances in colloidal photonic crystal sensors: Materials, structures and analysis methods," *Nano Today*, Vol. 22, 132–144, 2018, doi: 10.1016/j.nantod.2018.08.008.
31. Gedney, S. D., *Introduction to the Finite-Difference Time-Domain (FDTD)) Method for Electromagnetics*, Vol. 27, 2011, doi: 10.2200/S00316ED1V01Y201012CEM027.
32. De Raedt, H., K. Michielsen, J. S. Kole, and M. T. Figge, "One-step finite-difference time-domain algorithm to solve the Maxwell equations," *Phys. Rev. E — Stat. Physics, Plasmas, Fluids, Relat. Interdiscip. Top.*, Vol. 67, No. 5, 12, 2003, doi: 10.1103/PhysRevE.67.056706.
33. Rajasekar, R., G. Thavasi Raja, and S. Robinson, "Numerical analysis of reconfigurable and multifunctional barium titanate platform based on photonic crystal ring resonator," *IEEE Trans. Nanotechnol.*, Vol. 20, 282–291, 2021, doi: 10.1109/TNANO.2021.3069401.
34. Purnamaningsih, R. W., N. R. Poespawati, T. Abuzairi, and E. Dogheche, "An optical power divider based on mode coupling using GaN/Al2O3 for underwater communication," *Photonics*, Vol. 6, No. 2, 2019, doi: 10.3390/photonics6020063.
35. Boulesbaa, M., M. E. Hathat, A. Bounegab, and O. Oulad Haddar, "Improvement of optical characteristics of silicon based 1×3 beam splitter with photonic crystal waveguide," *AIP Conference Proceedings*, Vol. 2440, No. 1, 2022, 020001, doi: https://doi.org/10.1063/5.0075004.